

A&A manuscript no.
(will be inserted by hand later)

Your thesaurus codes are:
06(19.3)

ASTRONOMY
AND
ASTROPHYSICS

May 18, 1998

Temperature mapping of sunspots and pores from speckle reconstructed three colour photometry

P. Sütterlin and E. Wiehr

Universitäts-Sternwarte, Geismarlandstr. 11, D-37083 Göttingen, Germany

Received 2 March 1998 / Accepted 14 May 1998

Abstract. The two-dimensional temperature distribution in a highly structured sunspot and in two small umbrae is determined from a three-colour photometry in narrow spectral continua. Disturbing influences from the earth's atmosphere are removed by speckle masking techniques, yielding a spatial resolution limited by the telescope's aperture. The corresponding colour temperatures are consistent over a range of more than 2000 K, although the numerical correction introduced by the reconstruction differs largely for the three colours.

Part of the scatter in the temperature relation disappears when convoluting the final images with artificial PSFs that compensate for the different, colour dependent spatial resolution. The remaining spread in the scatter plots does not reflect noise, but is related to local variations of the temperature difference between the continuum emitting layers. This is most obvious for a small umbra which yields 'branches' in the scatter plots the 'bluer' of which corresponding to the limb-side umbral border. Here, the 'hot rim' of a Wilson depressed umbra becomes visible.

The temperature map of the large spot shows that the bright umbral dots do not reach the temperature of the non-spot surroundings. Instead, they exceed the 2000 K cooler umbral temperature minimum by 900-1300 K. The filamentary structure of the surrounding penumbra has spatial temperature fluctuations of typically 700 K, a value which fits earlier observed contrasts. However, the mean temperatures of 5650 K in the dark and 6250 K in the bright penumbral fine structures exceed former findings. Exceptionally bright penumbral grains are 250 K than the mean solar surface and thus exceed even brightest granules.

Key words: sunspots – intensity – temperature

1. Introduction

The increasing spatial resolution achieved in solar observations impressively demonstrates that neither the magnetic field nor the atmosphere of active region phenomena can be assumed as homogeneous. Instead, the fine-structure plays an essential role for the existence of sunspots, plages or prominences.

Correspondence to: ewiehr@uni-sw.gwdg.de

Their observation requires a spatial resolution near $0''.1$ and is thus strongly influenced by disturbances from the earth's atmosphere. These can be largely reduced by numerical image restoration techniques. The resulting two-dimensional images allow the investigation of 'dynamical quantities' like e.g. lifetimes and lateral motions (de Boer et al. 1992; de Boer & Kneer 1992; Denker et al. 1995) which agree with findings from frame selected best images (Dunn & Zirker 1973; Muller 1973; Koutchmy & Adjabshirzadeh 1981; Shine et al. 1994). In contrast, other parameters like magnetic field, gas pressure, turbulence, line-of-sight velocity require spectroscopy which, until now, has not succeeded to resolve individual fine-structures of $< 0''.2$ diameter. The temperature, however, can be deduced at an adequate spatial resolution from two-dimensional multi-colour photometry (Koutchmy & Adjabshirzadeh 1981; Grossmann-Doerth et al. 1986).

These earlier observations are now improved by observing simultaneously at three wavelengths in continuum windows free of spectral lines, and by applying speckle techniques to remove the wavelength-dependent influence of atmospheric disturbances. The final images in three colours can be used to check the quantitative character of the reconstruction procedure and to derive actual temperatures of the sunspot fine structures at a spatial scale near 100 km on the solar surface.

2. Observations

For this purpose, small-band interference filters were used to select three continua at 450.6 ± 0.15 nm, 658.7 ± 0.35 nm, and 863.5 ± 0.5 nm. We verified by spectroscopic inspection that these windows are not significantly affected by absorption lines as far as the undisturbed solar surface is concerned. However, this does not hold for sunspot umbrae (see e.g. Stellmacher & Wiehr 1970). The three colours were observed simultaneously using beam splitters at the 0.7 m Vacuum Tower Telescope on Tenerife. The read-out of the three 1024×1024 CCD cameras was restricted to sub-fields of 286×384 pixels, which is sufficiently large to cover the sunspot, but small enough for a short repetition time. At an integration time of 5 ms, a burst of 50 images took 100 sec, which is fast enough with respect to the typical life-times of the sunspot structures. The scale of

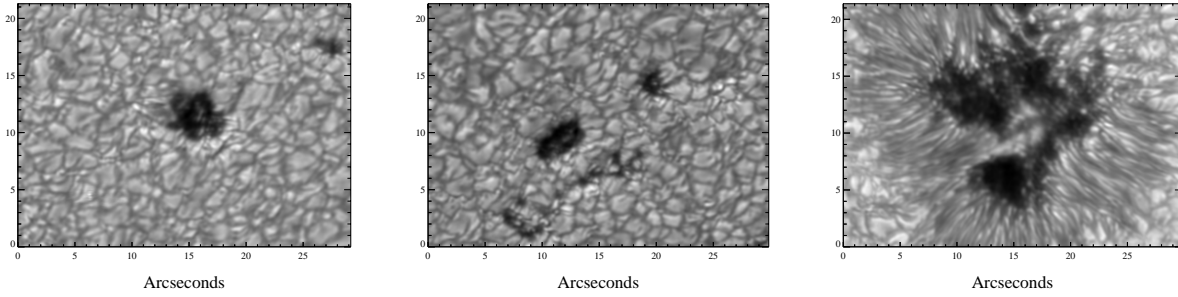


Fig. 1. Speckle reconstructed images from May 19, 1997, in the blue continuum at 450.6 ± 0.15 nm of (a,b) small spots and pores at $\vartheta \approx 40^\circ$ and (c) a large spot at $\vartheta \approx 20^\circ$.

$0''.086/\text{pixel}$ corresponds to 62 km on the solar surface, yielding a limit for the spatial resolution of 125 km.

A large sunspot at a heliocentric angle of $\vartheta \approx 20^\circ$ and a group of small spots without penumbra at $\vartheta \approx 40^\circ$ were observed on May 19, 1997, (cf. Fig. 1) under good seeing conditions. The 50 images of each burst were numerically treated by the speckle masking method (Weigelt & Wirtzner 1983; de Boer 1995) in order to remove the wavelength dependent influence of seeing, as indicated by the actual Fried parameters of $R_0 = 8.7, 14.1,$ and 20.6 cm for the three continua. The resulting spatial resolution corresponds to 95 (limited by our binning to 125), 145, and 180 km on the solar surface. For a point-to-point comparison of the final three images, lateral shifts, rotations, and individual scales were carefully adapted. This procedure slightly reduces the spatial area available for the temperature mapping.

Observations of sunspots are known to be strongly affected by parasitic light, the majority of which is caused by image motion and blurring. Both are removed by our image processing. The remaining scattered light can be estimated to approximately 2% for the recently aluminized mirrors of the VTT (cf. Stellmacher & Wiehr 1970). Such an error leads to an overestimate of ≤ 50 K in the darkest umbral nucleus.

The local intensities are calibrated in terms of the mean undisturbed solar surface intensity, using the absolute values of Labs & Neckel (1984) and their center-to-limb variations (Pierce & Slaughter 1977a,b). The resulting intensities in the three continua can be converted into brightness temperatures via the Planck law.

3. Comparison of the three brightness temperatures

The scatter plots of the brightness temperatures of each location in and outside the sunspots show that the ‘blue temperatures’ exceed the ‘red’ ones by a constant offset of ~ 270 K (Fig. 2a), whereas the ‘infrared temperatures’ are ~ 65 K lower (Fig. 2b). If we accordingly correct the blue and the infrared temperatures for those offsets, the three continuum images yield consistent temperatures from darkest umbral cores to bright penumbral grains. Only the brightest penumbral grains and granules show a slightly larger blue temperature excess.

The finding of largely constant offsets is, at a first glance, astonishing, since one might expect a dependence on the

brightness of the different structures due to their different temperature gradients and opacities. However, the almost parallel colour curves of the continuous absorption coefficient, κ_{H-} , for different temperatures (Böhm-Vitense 1965) cause that the relative differences between the κ_{H-} for the three wavelengths are nearly temperature-independent. We checked this behaviour by calculations with empirical models assuming the photospheric stratification by Holweger & Müller (1974) for the bright structures, and for the darkest umbral cores the model by Kollatschny et al. (1980). These two models yield continuum intensities for the three colours which correspond to brightness temperatures of 6440, 6150, 6075 K for the hot and 4230, 4030, 3980 K for the cool atmosphere. The temperature differences of $\Delta T^{\text{hot}} = 365$ K and $\Delta T^{\text{cool}} = 250$ K well fit our observed mean value of $270 + 65 = 335$ K. The calculations furthermore show that the three continua span a formation range of $\Delta \log \tau_{500}^{\text{hot}} = 0.23$ and $\Delta \log \tau_{500}^{\text{cool}} = 0.30$. The smaller value for the hot atmosphere largely counterbalances its steeper temperature gradient thus yielding the rather similar ΔT values. As a consequence, the difference of the brightness temperatures in our three continua is largely independent from the local structure brightness.

The scatter of the data points (Fig. 2a and b) is partly due to the different spatial resolution in the three images. We removed these effects by convoluting the images with artificial modulation transfer functions, MTF, that compensate these differences in resolution and produce images that have a resolution slightly below that of the IR image, i.e. 180 km. This procedure reduces the spread of the data points (Fig. 2c). It also reveals a ‘branching’ for some areas which is most pronounced in the temperature regime $5500 < T_{\text{red}} < 5800$ K. Close inspection shows that the data points from the upper branch correspond to the limb-side, those from the lower branch to the center-side of the umbral rim (cf. Fig. 3). Branches also occur at the ‘hot ends’ of the scatter plots. Here, the upper branch corresponds to local brightenings in the spot surroundings.

We checked that also those parts of the scatter plots which do not show a pronounced branching are related to specific locations in the images. This indicates that the remaining spread in the scatter plots (Fig. 2c) does not reflect noise of the data. Instead, locations with higher blue temperatures at given red (or IR) temperatures reflect local temperature differences between the layers which emit the corresponding continua, i.e. different

temperature gradients. These become visible if smaller opacity yields radiation from deeper layers where the temperature gradient is larger. This seems to be the case at the limb-side umbral border where the hot sunspot surroundings are seen through the Wilson depressed spot atmosphere. The local brightenings in the spot surroundings, producing the upper branch of the ‘hot ends’ in Fig. 2c, may be the signature of facular grains which are known to become visible in the continuum just at this heliocentric distance (cf. Muller 1973). The lateral view into these hot structures may be the reason for the enhanced blue temperature.

4. Temperature of the fine-structures

The finally deduced temperature map for the large spot (Fig. 4) shows that the three dark umbral nuclei have brightness temperatures of 4360, 4570, and 4630 K, which are significantly higher than those of the model for darkest umbral cores (Kollatschny et al. 1980). This supports the finding by Sobotka et al. (1993) that the dark sunspot background varies from one spot to the other and determines the mean umbral brightness rather than individual filling with dots, as was discussed by Stellmacher & Wiehr (1985).

Among a selected number of well defined umbral dots, none reaches photospheric temperatures; they typically exceed the umbral minimum temperature by 900-1300 K. The faint dots near the umbral centres have temperatures of about 5250 K; the brighter dots at the umbral periphery range up to 5650 K. Two exceptional bright regions of 5937 K and 6124 K are part of lightbridge-like structures or ‘inner penumbral grains’; but even these do not reach the photospheric brightness temperature. This result confirms spectroscopic results of Tritschler & Schmidt (1997) who find reduced brightness temperatures for central ($\sim 30\%$) and peripheral (20 – 25%) dots. However, the temperature excess of 900 K in umbral dots fits the mean observed brightness ratio of 2.6 at 542.5 nm between dots and their neighbourhood (Sobotka et al. 1993). The spread of 900-1300 K may reflect a temporal mean of evolving dots (Koutchmy & Adjabshirzadeh 1981)

The sunspot penumbra shows spatial temperature fluctuations of typically 700 K corresponding to an intensity contrast slightly below the 1.6 value observed at 550 nm (Muller 1973). The darkest penumbral filaments have temperatures similar to those of the brightest umbral dots. This corresponds to 0.64 of the photospheric brightness in the continuum at 550 nm and exceeds the observed range of 0.52-0.6 (Muller 1973) adopted for fine-structure models (Kjeldseth-Moe & Maltby 1974), but agrees with del Toro Iniesta et al. (1994). Brighter penumbral grains are about 100 K hotter than the mean photosphere and thus above the values by Muller (1973) and by del Toro Iniesta et al. (1994). A few exceptionally bright penumbral grains exceed the 6400 K level, thus being hotter than the brightest granules.

For the spatially averaged penumbra, we find a brightness temperature of 5850 K, corresponding to a contrast of 0.75 at 550 nm (0.6, 0.8, 0.89 in our continua), which is in good

agreement with observed mean penumbral contrasts (Maltby & Mykland 1969). This supports the quantitative character of temperatures deduced from speckle reconstructed continuum images, in agreement with a recent study of the temperature excess in solar limb faculae by de Boer et al. (1997).

Acknowledgements. We thank Drs. C.R. de Boer and G. Stellmacher for interesting discussions. The Vacuum Tower Telescope on Tenerife island, VTT, is operated by the Kiepenheuer Institut für Sonnenphysik, Freiburg, at the Spanish Observatorio del Teide of the Instituto de Astrofísica de Canarias.

References

- Böhm-Vitense, E.: 1965, in *Landold-Börnstein Vol.1* (ed. H. H. Voigt), Springer-Heidelberg
- de Boer, C.R.: 1995, *A&AS* 114, 387
- de Boer, C.R., Kneer, F., Nesis, A.: 1992, *A&A* 257, L-4
- de Boer, C.R., Kneer, F.: 1992, *A&A* 264, L-24
- de Boer, C.R., Stellmacher, G., Wiehr, E.: 1997, *A&A* 324, 1179
- del Toro Iniesta, J.C., Tarbell, T.D., Ruiz Cobo, B.: 1994, *ApJ*, 436, 400
- Denker, C., de Boer, C.R., Volkmer, R., Kneer, F.: 1995, *A&A* 296, 567
- Dunn, R.B., Zirker, J.B.: 1973, *Solar Phys.* 33, 281
- Grossmann-Doerth, U., Schmidt, W., Schröter, E.H.: 1986, *A&A* 156, 347
- Holweger, H., Müller, E.A.: 1974, *Solar Phys.* 39, 19
- Kjeldseth-Moe, O., Maltby, P.: 1974, *Solar Phys.* 36, 101
- Kollatschny, W., Stellmacher, G., Wiehr, E.: 1980, *A&A* 86, 245
- Koutchmy, S., Adjabshirzadeh, A.: 1981, *A&A* 99, 111
- Labs, D., Neckel, H.: 1984, *Solar Phys.* 90, 205
- Maltby, P., Mykland, N.: 1969, *Solar Phys.* 8, 23
- Muller, R.: 1973, *Solar Phys.* 32, 409
- Pierce, A.K., Slaughter, C.D.: 1977a, *Solar Phys.* 51, 25
- Pierce, A.K., Slaughter, C.D.: 1977b, *Solar Phys.* 52, 179
- Shine, R.A., Title, A.M., Tarbell, T.D., Smith, K., Frank, Z.A., Scharmer, G.: 1994, *ApJ* 430, 413
- Stellmacher, G., Wiehr, E.: 1970, *A&A* 7, 432
- Stellmacher, G., Wiehr, E.: 1985, in *8th Europ. IAU/EPS meeting on High Resolution in Solar Physics* (ed. R. Muller), p.254
- Sobotka, M., Bonet, J.A., Vázquez, M.: 1993, *ApJ* 415, 832
- Tritschler, A., Schmidt, W.: 1997, *A&A* 321, 643
- Weigelt, G., Wirtzner, B.: 1983, *Optics Letters* Vol.8, No.7, 389

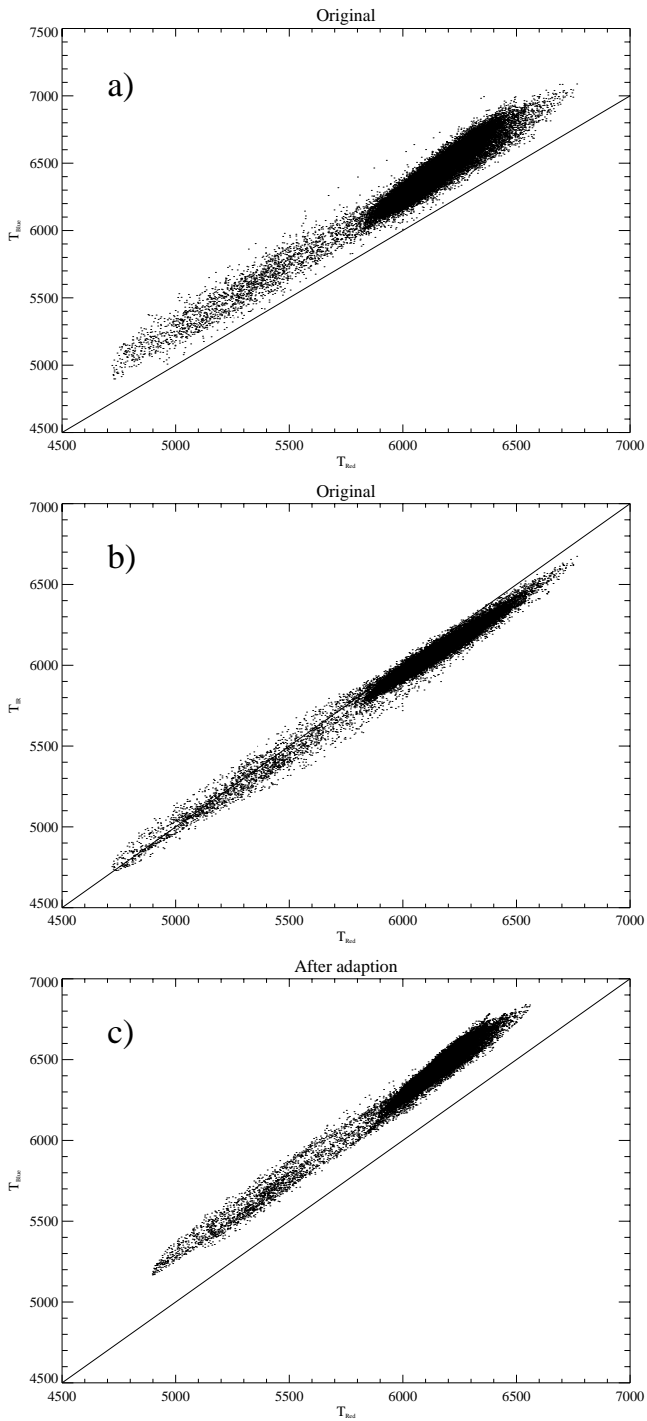


Fig. 2. Scatter plot of observed brightness temperatures for the small sunspot at $\vartheta \approx 40^\circ$ (a in Fig. 1). Abscissa: temperatures from the red continuum image; ordinate: temperatures from the blue (a) and the infrared (b) continuum images for all locations inside and outside the spot; (c) like (a) but after convolution with an artificial PSF to compensate the colour dependent spatial resolution.

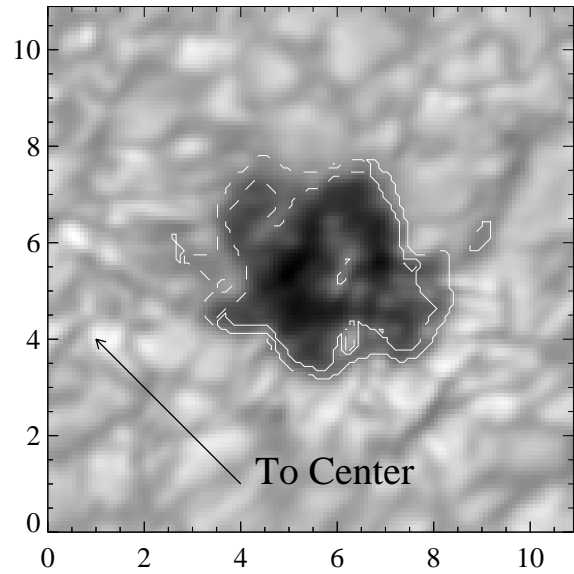


Fig. 3. Location of the two branches visible in the scatter plot c) of Fig. 2. The dash-dotted line marks the areas where – at the same temperature in the red continuum – the 'blue' temperature is reduced, the solid line encircles the area with higher blue temperatures, which are located at the limb-side umbral edge.

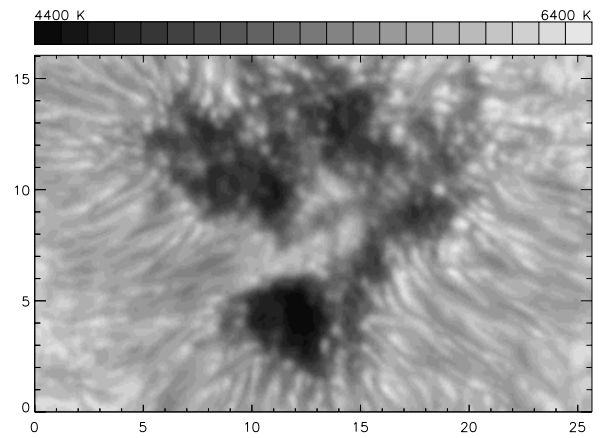


Fig. 4. Temperature map for the large sunspot at $\vartheta \approx 40^\circ$.